

# Multiple Source Cooperation: From Code Division Multiplexing To Variable-Rate Network Coding

Rong Zhang and Lajos Hanzo

School of ECS, Univ. of Southampton, SO17 1BJ, UK.

Tel: +44-23-80-593 125, Fax: +44-23-80-593 045

Email: rz,lh@ecs.soton.ac.uk, <http://www-mobile.ecs.soton.ac.uk>

**Abstract**—Multiple Source Cooperation (MSC) techniques, including conventional Code Division Multiplexing (CDM) and Classic Network Coding (CNC) are investigated. We adopt a soft sum-product decoding algorithm for the CNC technique for efficiently processing a large number of information streams and propose a flexible Variable-rate Network Coding (VNC) technique, which is capable of attaining a near-optimum performance. Quantitatively, the proposed VNC method is capable of operating within 1dB from the outage capacity of the quasi-static Rayleigh fading channel. The iterative decoding convergence of the multiple source computation methods is analysed with the aid of EXtrinsic Information Transfer (EXIT) charts.

## I. INTRODUCTION

Cooperative communications attracted substantial research interests in recent years [1]–[4], spanning from the classic single-source single-relay scenario [5] to the generalised Multiple Source Multiple Relay (MSMR) scenario [6]. When considering the MSMR network topology, a fundamental issue is the efficient processing of numerous source information streams during their relaying [7].

The processing of multiple sources may be treated analogously to the classic multiplexing problem, which may be based either on an orthogonal or on a non-orthogonal Code Division Multiplexing (CDM) approach [8]. Specifically, the information-theoretically attractive superposition modulation aided multiple source cooperation scenario was considered in the context of two sources in [9] and for multiple sources in [10]. On the other hand, the relay may generate the 'XOR'ed information of the multiple source streams in the context of both the original bit-based Classic Network Coding (CNC) scheme [11], [12] and in the modified waveform-based Physical-layer Network Coding (PNC) arrangement [13], [14]. It is worth noting that the concept of both CDM and of CNC may be considered as a *modulation* technique, where the former scheme is implemented using arithmetic additions in the complex-valued domain, while the latter scheme is realised using modulo additions over the finite Galois field.

On the other hand, a coding-related interpretation may also be conceived for both CNC and PNC, because both techniques

impose a certain constraint, which is reminiscent of channel coding. Since the decoding (demapping) of CNC (PNC) for a large number of source information streams is non-trivial, the CNC and PNC concept is pre-dominantly used in cooperative scenarios when the number of source information streams is small. This specific scenario is encountered in two-way communications [15], [16] or for transmission over twin-source multiple access relay channels. To take a further step forward, the so-called joint channel and network coding [16] or multiplexed coding [17], [18] concept was proposed in order to provide an additional channel coding gain by imposing carefully designed redundancy, where the sources' information streams are treated as a single amalgamated stream, before it is channel encoded.

Since extensive research efforts have been dedicated to two-way communications, in this paper, we focus our attention on the efficient processing of the multiple source information streams in the context of Multiple Source Cooperation (MSC) [19]–[21], which constitutes a specific instantiation of the MSMR scenario, where the relays are also active sources. MSC was first considered in [19], where the authors proposed the so-called parity-check based MSC regime using Reed-Solomon (RS) codes to jointly encode the multiple information streams at the relay. On the other hand, the authors of [20] proposed the so-called Complex Field Coding (CFC) aided MSC, where the multiple source information streams are combined in a specific way in order to yield values in the complex field. Furthermore, it was reported in [20] that the CFC aided MSC is capable of achieving both the maximum attainable diversity order and a high spectral efficiency. When compared to the parity-check MSC of [19], the authors of [20] claimed that the full diversity gain provided by CFC aided MSC is to an extent capable of compensating for its modest channel coding gain. However, the Bit Error Ratio (BER) results presented in [20] are not directly characteristic of the channel coding gain attainable in quasi-static Rayleigh fading channels. Hence, in [10], we proposed a high throughput MSC framework and extended it to a multiplexed coding regime with the aid of a Low Density Generator Matrix (LDGM) based design [21].

Apart from the sophisticated joint channel and network coding schemes proposed in the literature for MSC that rely on a channel code, the performance of the pure CNC scheme has not been explored in the context of MSC. Firstly, this is because the decoding of a particular information stream

Copyright (c) 2010 IEEE. Personal use of this material is permitted. However, permission to use this material for any other purposes must be obtained from the IEEE by sending a request to [pubs-permissions@ieee.org](mailto:pubs-permissions@ieee.org).

Acknowledgements: The financial support of the EPSRC under the auspice of the UK-India Centre of Excellence in Wireless Communications is gratefully acknowledged.

$x_a$  from the composite CNC stream of  $x_a \oplus x_b \oplus x_c \oplus \dots$  requires the knowledge of the correct 'XOR'ed information of all the rest of the network's information streams, namely of  $x_b \oplus x_c \oplus \dots$ . However, unlike in two-way communications, this knowledge is not readily available in MSC at the destination. Furthermore, the mapping ambiguity of CNC, which is represented by  $x_a \oplus x_b \oplus x_c \oplus \dots = x_c \oplus x_b \oplus x_a \oplus \dots$ , prevents its employment in MSC, as also stated in [20], which was one of the main motivations of conceiving their CFC. Hence, in order to overcome this problem, in this paper:

- we consider a range of multiple source processing techniques, ranging from the basic CDM concept to the CNC technique.
- we conceive the soft decoding of CNC with the aid of factor graphs, which is capable of reliable operation even in the presence of unreliable network information streams  $x_b \oplus x_c \oplus \dots$ .
- we also propose a novel Variable-rate Network Coding (VNC) regime<sup>1</sup> that is capable of operating near capacity without necessitating a sophisticated joint channel and network code design.

We organise our paper as follows. In Section II, we describe the two-phase transmissions aided MSC regime considered and introduce a range of multiple source stream processing methods, including CDM, CNC and the proposed VNC. The corresponding iterative receiver algorithms are provided in Section III, while our EXIT chart analysis is detailed in Section IV. Finally, we present our simulation results in Section V and conclude in Section VI. To assist the presentation of this paper, important symbols and frequently used abbreviations are listed in Table I and Table II.

## II. SYSTEM DESCRIPTION

### A. Cooperation Scenario

1) *Overview*: Let us consider a cooperation scenario involving  $K$  sources and a single destination  $D$ , where these  $K$  sources form a cluster for cooperatively transmitting their information to the destination. All  $K$  sources in the cluster are assumed to have the same distance from the destination and they are allocated close to each other within the cluster. Since a node is unable to simultaneously transmit and receive, we assume Time Division Duplexing (TDD) in our paper. We assume furthermore that both the  $K$  sources and the destination employ a single antenna and all transmissions are perfectly synchronised.

In the first transmission phase, each of the  $K$  sources sends its information within the  $K$  orthogonal channels constituted by  $K$  non-overlapping time slots to the destination as well as to the rest of the sources that are listening as seen in Fig 1. After the first information exchange phase, all of the  $K$

<sup>1</sup>The authors of [22] considered a single source multicast application scenario, where the data flow at the intermediate node may be subject to different rate requirements and the authors of [22] focus their attention on the associated flow control. Hence, the terminology of *variable rate* in [22] has no overlap with that of the current paper, since in the latter, we design a physical layer network coding scheme in conjunction with advanced channel coding techniques in order to flexibly adapt the rates of the resultant network coding streams in a MSC framework.

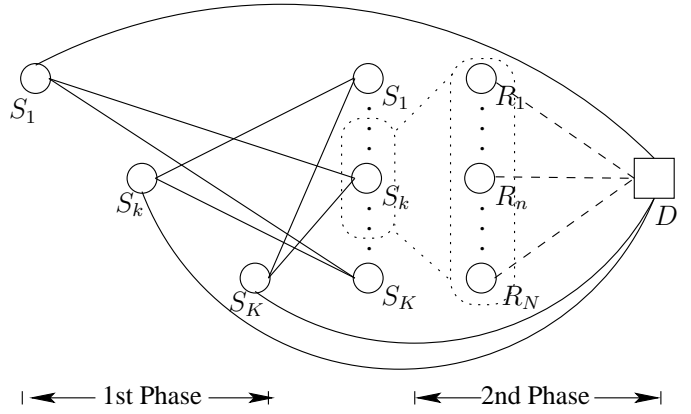


Fig. 1. Schematic of  $K$  sources cooperation employing TDD. First phase transmission employs orthogonal TDMA and second phase transmission employs non-orthogonal multiple access, where dotted block represents the relay cluster  $1 < N \leq K$ .

sources have access to all the information within the cluster. In the second transmission phase,  $1 < N \leq K$  sources form a relay cluster, where each of the  $N$  relays exploits all the information available in the cluster *distributively* and transmits the appropriately processed information of the  $K$  sources to the destination *simultaneously* with the transmissions of all the  $(N - 1)$  other relays for the sake of achieving a high cooperation efficiency, as seen in the multiple access channel model of Fig 1. Finally, the information received during the two phases is jointly processed at the destination before making a hard decision.

2) *First Phase Cooperation*: We commence by considering the first phase of the  $k$ th source  $S_k$ , where the information bit vector of length  $N_b$  is denoted by  $\mathbf{b}_k^I$ . Following channel coding and modulation, we generate the transmit data vector  $\mathbf{x}_k^I$  of length  $N_x$ . Thus, the discrete time baseband system's first phase model of source  $S_k$  describing its transmission to the destination as well as to relay  $n$  are given by:

$$\mathbf{y}_D^I = h_{k,D}^I \mathbf{x}_k^I + \mathbf{n}_{k,D}^I, \quad \mathbf{y}_n^I = h_{k,n}^I \mathbf{x}_k^I + \mathbf{n}_{k,n}^I, \quad k \neq n \quad (1)$$

where  $\mathbf{y}_D^I$  and  $\mathbf{y}_n^I$  denote the received signal vector of length  $N_x$  at the destination and at the  $n$ th relay, respectively. Furthermore,  $h_{k,D}^I$  and  $h_{k,n}^I$  denote the quasi-static flat Rayleigh fading channel between source  $k$  and the destination as well as between source  $k$  and relay  $n$ , respectively. Finally,  $\mathbf{n}_{k,D}^I$  and  $\mathbf{n}_{k,n}^I$  denote the complex-valued Additive White Gaussian Noise (AWGN) vector of length  $N_x$ .

The signal  $\mathbf{y}_D^I$  received at the destination will be jointly processed in conjunction with the signal  $\mathbf{y}_D^{II}$  received at the destination during the second phase to be introduced below. On the other hand, the signal  $\mathbf{y}_n^I$  received at relay  $n$  is first decoded and then prepared for the second transmission phase.

*Remark 1* There are numerous solutions that deal with the decoding errors of the first phase at the relay, when employing the Decode-and-Forward (DF) technique [23]. However, we focus our attention exclusively on the MSC techniques used at the relays and set aside the issue of decoding error countermeasures for future research. We first consider the *error-free* relaying scenario, where no first-phase decoding errors

are encountered. Secondly, we consider the potentially *error-infested* scenario, where there may be decoding errors at the relays and these errors are characterized by the associated bit error probabilities, regardless of the specific baseband schemes employed during the first transmission phase.

3) *Second Phase Cooperation*: Let us now consider the operation of relay  $n$ , which has access to all the information in the cluster that may be collectively represented as  $\{\tilde{\mathbf{b}}_{n,1}^I, \dots, \tilde{\mathbf{b}}_{n,K}^I\}$ , where  $\tilde{\cdot}$  denotes the estimated version of the parameter, which is potentially erroneous, with the exception of  $\tilde{\mathbf{b}}_{n,n}^I = \mathbf{b}_{n,n}^I$ . Relay  $R_n$  then performs the operations to be detailed in Section II-B and generates the resultant transmit data vector as  $\mathbf{x}_n^{II}$  of length  $N_x$ . Hence the discrete time baseband system model of the concurrent second phase transmissions of the  $N$  relays to the destination is formulated as:

$$\mathbf{y}_D^{II} = \sum_{n=1}^N h_{n,D}^{II} \mathbf{x}_n^{II} + \mathbf{n}_D^{II}, \quad (2)$$

where  $\mathbf{y}_D^{II}$  denotes the received signal vector of length  $N_x$  at the destination and  $h_{n,D}^{II}$  denotes the quasi-static flat Rayleigh fading channel between relay  $n$  and the destination. Furthermore,  $\mathbf{n}_D^{II}$  denotes the complex-valued AWGN vector of length  $N_x$ .

*Remark 2* Since two-phase MSC is employed,  $P^I$  and  $P^{II}$  denote the total transmission power available for the first and second phase, respectively, where we let  $P^I = P^{II} = P/2$ , where  $P$  is the total available power that is normalised to unity. Furthermore,  $P_n = P^{II}/N$  denotes the total transmit power of relay  $n$  that is assumed to be equally shared. We stipulate this equal-power assumption based on the argument that requiring Channel State Information (CSI) at multiple relays is often considered too demanding. Even in the presence of CSI, the allocation of power amongst multiple relays typically requires a centralised controller and sophisticated signal processing.

## B. Computation Methods At Relay

Let us first define the normalised throughput per relay node as  $\eta = Krb/W$ , where  $r$  is the channel coding rate,  $b = 1$  is the number of bits per symbol assuming BPSK modulation and  $W$  is the total number of orthogonal channels required to convey  $K$  sources' information by the relay node. When  $W = K$  orthogonal channels are considered, the normalised throughput per relay node is  $\eta_o = r$ .

1) *Code Division Multiplexing*: Non-orthogonal CDM refers to the transmission of  $K$  bit vectors using  $K$  unique non-orthogonal *codes*, each viewed as a layer reminiscent of superposition modulation [9], where the codes may be constructed by a *source-specific* channel code or interleaver.

As seen in Fig 2, at relay  $n$ , each of the  $K$  bit vectors is first channel coded by a stream-specific coding function  $f_{c,k}$  to yield a length- $N_c$  coded bit vector  $\mathbf{c}_{n,k}^{II}$  and then BPSK modulated, as characterized by the function  $f_m$ , in order to yield a length- $N_c$  modulated data vector  $\mathbf{x}_{n,k}^{II}$ . Finally, the resultant  $K$  modulated data vectors are superimposed at relay  $n$  in order to form the composite transmit data vector  $\mathbf{x}_n^{II}$  of

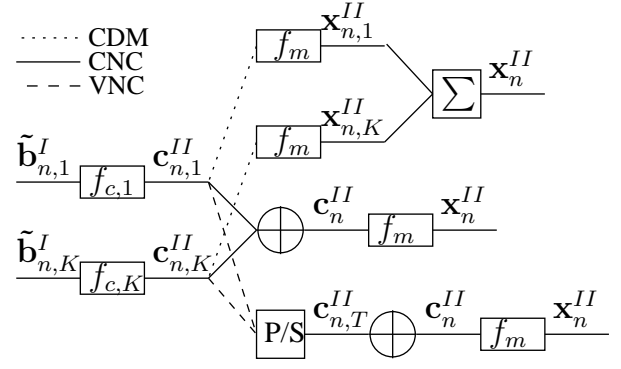


Fig. 2. Various multiple source computation methods at relay.

length  $N_c$ , which may be represented by:

$$\mathbf{x}_n^{II} = \sum_{\forall k} \rho_k \mathbf{x}_{n,k}^{II} = \sum_{\forall k} \rho_k f_m[f_{c,k}(\tilde{\mathbf{b}}_{n,k}^I)], \quad (3)$$

where  $\rho_k = \sqrt{P_n/K}$  is the equally shared transmit power of the  $k$ th non-orthogonal code-based channel and the possibility of unequally allocating the power  $\rho_k$  is beyond the scope of our paper. Moreover, it is vital for non-orthogonal CDM to have stream-specific channel codes to ensure the unique distinction of the  $K$  superimposed layers, where we opted for employing stream-specific random interleavers  $\pi_k$ . Hence, the normalised throughput per relay node in the CDM scenario considered is  $\eta_{cdm} = Kr$ .

2) *Element-wise Bit-level CNC*: In its simplest guise, CNC transmits  $K$  bit vectors per composite channel, which contains the 'XOR'ed function of the  $K$  bit vectors, rather than transmitting the  $K$  bit vectors themselves. To expound a little further, combining the multiple information streams may be carried out in terms of their sampled analogue waveform or in terms of the bit-based streams. The former leads to PNC, while the latter is deemed to be the CNC. Since the PNC requires a sophisticated waveform-to-bit mapping scheme, it is only considered practical for a low number of information streams. Given the limited scalability of PNC and that in the context of MSC, we typically consider a large value of  $K$ , we opt for using the element-wise bit-level CNC and propose a novel packet-wise bit-level VNC scheme.

In the CNC scheme of Fig 2, each of the  $K$  information bit vectors is first subjected to stream-specific channel coding at relay  $n$ , yielding the coded bit vector  $\mathbf{c}_{n,k}^{II}$  of length  $N_c$ . These  $K$  coded bit vectors are then element-wise 'XOR'ed to yield a composite CNC bit vector  $\mathbf{c}_n^{II}$  of length  $N_c$ . Finally, the CNC bit vector  $\mathbf{c}_n^{II}$  is BPSK modulated by the function  $f_m$  in order to form the length- $N_c$  transmit data vector  $\mathbf{x}_n^{II}$ . Mathematically, we have:

$$\mathbf{x}_n^{II} = f_m[\mathbf{c}_n^{II}] = f_m\left[\bigoplus_{\forall k} \mathbf{c}_{n,k}^{II}\right] = f_m\left[\bigoplus_{\forall k} f_{c,k}(\tilde{\mathbf{b}}_{n,k}^I)\right]. \quad (4)$$

Note that the normalised throughput per relay node of the CNC scheme is also  $\eta_{cnc} = Kr$ .

In the sequel, we assume that the readers are familiar with the basics of factor graphs [24]. Since CNC may be viewed as the element-wise parity check of the  $K$  coded bit vectors, the

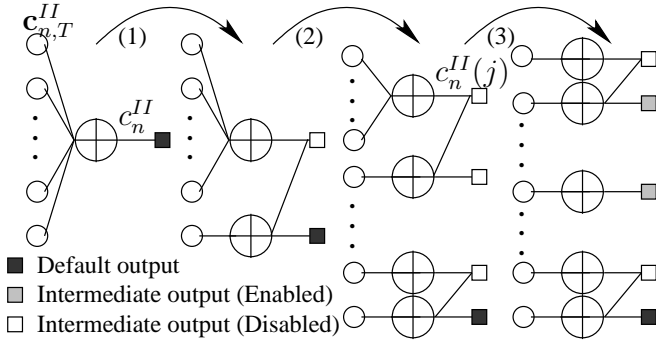


Fig. 3. Factor graph of packet-wise bit-level VNC, where the left subplot shows the graph of  $r_\infty$ -VNC, the middle two subplots show the transition graph of  $r_\infty$ -VNC and the right subplot shows the ultimately transformed graph of general VNC with two enabled intermediate outputs.

associated 'XOR' operation may be interpreted as the action of a check node of degree  $d_c = K$ , which has  $K$  incoming edges and a single outgoing edge. It is then natural for us to explore the possibility of increasing the check node degree, which leads to our proposed packet-wise bit-level VNC scheme.

3) *Packet-wise Bit-level VNC*: We now introduce our packet-wise bit-level VNC scheme seen in Fig 2. At relay  $n$ , the  $K$  stream-specific coded bit vectors  $\mathbf{c}_{n,k}^{II}, \forall k$  are Parallel to Serial (P/S) converted to yield a concatenated coded bit vector  $\mathbf{c}_{n,T}^{II}$  of length  $KN_c$ , obeying  $c_{n,T}^{II}(i) = c_{n,a_1}^{II}(a_2)$  with  $a_1 = [(i-1) \bmod K] + 1$  and  $a_2 = \lceil i/K \rceil$ , where  $\lceil \cdot \rceil$  represents the largest integer operator. Then the 'XOR' operation is performed for all the parallel bits of  $\mathbf{c}_{n,T}^{II}$  (packet-wise) in order to yield a single bit  $c_n^{II}$ , as seen at the left of Fig 3. This is then followed by the BPSK modulation, as described by the function  $f_m$ . Hence, we have

$$x_n^{II} = f_m(c_n^{II}) = f_m\left[\bigoplus_{i=1}^{KN_c} c_{n,T}^{II}(i)\right]. \quad (5)$$

Again, the left subplot of Fig 3 portrays the operation in Eq (5), where the  $KN_c$  bit inputs (variable nodes) of  $\mathbf{c}_{n,T}^{II}$  denoted by circles are combined with the aid of their XOR operation, which we refer to as being CNC checked (check node), which are denoted by the crossed-circle symbol in order to yield a single-bit output  $c_n^{II}$  denoted by the filled square symbol.

To elaborate further, sending only the CNC checked bit results into an extremely compressed packet, since only a single bit is transmitted by the relay. Insightfully, we may transform however the resultant single  $(KN_c + 1)$ -edge check node to  $KN_c$  three-edge check nodes, as seen in stages (1), (2) and (3) of Fig 3. The final transformed graph is then seen in the right subplot of Fig 3. This transformation allows us to transmit any number of additional intermediate outputs, so that the extremely 'over-compressed' single-bit source packet is better separated, as seen in the right subplot of Fig 3, where two more outputs are seen to be enabled. Mathematically, the  $j$ th intermediate output may be written as:

$$c_n^{II}(j) = \bigoplus_{i=1}^j c_{n,T}^{II}(i) \quad j \in [1, KN_c]. \quad (6)$$

Let furthermore  $\Omega$  host the indices associated with the enabled outputs. Then the transmit data vector becomes  $\mathbf{x}_n^{II} = f_m[c_n^{II}(j)], \forall j \in \Omega$ .

By appropriately controlling the number of intermediate outputs, a conveniently controlled variable rate scheme arises. We thus refer to our proposed scheme as a VNC arrangement having a rate of  $r_v$ . Furthermore, we refer to the particular arrangement transmitting the single CNC checked bit representing all the  $KN_c$  bits as  $r_\infty$ -VNC and that transmitting all intermediate outputs as  $r_1$ -VNC, which correspond to  $\Omega = [1, KN_c]$ . Note that the normalised throughput per relay node is  $\eta_{vnc} = r_v r$ .

### III. ITERATIVE RECEIVER AT DESTINATION

#### A. Receiver Structure

Given the received signal observations of  $\mathbf{y}_D^I, \mathbf{y}_D^{II}$  and the knowledge of CSI, we employ iterative receiver [25] to pursue the Maximum *A posteriori* Probability (MAP) estimate of each source's information owing to the otherwise excessive complexity. Exchanging extrinsic information by iterating between the two receiver phases may be mutually helpful, but our focus is on the encoding and decoding techniques of the second transmission phase, hence we assume that the first phase source to destination transmission provides the second phase with a constant level of *a priori* mutual information of the multiple sources and will only discuss the iterative receiver of the second phase.

The iterative receiver of the second phase consists of four building blocks, as seen in Fig 4, which exchange Log-Likelihood Ratios (LLR) of the associated information. The first stage is the multiple relay based detection (DET), which separates the signals received from  $N$  relays. This is followed by the decomposition (DCP) of the  $K$  sources' information at each relay, where we collectively treat the decoding of each MSC technique as an instantiation of DCP. Each of the  $K$  decomposed information streams is then forwarded to the soft channel decoder (DEC) of Fig 4 associated with each of the  $K$  sources. Finally, maximum ratio combining (COM) of the  $N$  relays' signal is performed in order to achieve an improved decision by exploiting the diversity gain gleaned from the  $N$  replicas.

#### B. Receiver Algorithm

1) *Multiple Relay Detection*: The optimum calculation of *extrinsic* information generated by multiple relay aided detection requires exponentially increased computational complexity. In this paper, we employ a low-complexity interference cancellation type multiple relay detection algorithm [26]. When considering  $x_n^{II}$  for example, the low-complexity detector treats the interference contribution as Gaussian noise. Effectively, we have:

$$y_D^{II} = h_{n,D}^{II} x_n^{II} + \sum_{\forall m \neq n} h_{m,D}^{II} x_m^{II} + n_D^{II}. \quad (7)$$



particular, we have  $\mu^e[c_{n,T}^{II}(1)] = \mu_{v \rightarrow c}^0(1)$ ,  $\mu^a[c_{n,T}^{II}(1)] = \mu_{c \rightarrow v}^0(1)$  and  $\mu^e[c_n^{II}(KN_c)] = \mu_{c \rightarrow v}^0(KN_c)$ ,  $\mu^a[c_n^{II}(KN_c)] = \mu_{v \rightarrow c}^0(KN_c)$ . In the above message passing algorithm, the *a priori* LLRs  $\mu^a(c_{n,T}^{II})$  are the consequences of the P/S conversion of  $\mathcal{L}_{dcp}^a(c_{n,k}^{II})$ ,  $\forall k$  and the *extrinsic* LLRs  $\mu^e(c_{n,T}^{II})$  are further subject to S/P conversion in order to forward each  $\mathcal{L}_{dcp}^e(c_{n,k}^{II})$  value to the DEC block seen in Fig 4. On the other hand, as seen in Fig 4, the *a priori* LLRs  $\mu^a(c_n^{II})$  are generated from the *extrinsic* LLRs  $\mathcal{L}_{det}^e(c_n^{II}) = \mathcal{L}_{det}^e(x_n^{II})$  of the DET block of Fig 4 representing the BPSK demodulator, which are interpolated as zeros, wherever the intermediate outputs of the VNC scheme were blocked. Furthermore, the *extrinsic* LLRs  $\mu^e(c_n^{II})$  are fed back to the DET block of Fig 4 subject to enabling by the set  $\Omega$  in order to yield  $\mathcal{L}_{det}^a(c_n^{II})$  and hence we have  $\mathcal{L}_{det}^a(x_n^{II}) = \mathcal{L}_{det}^a(c_n^{II})$  for BPSK modulation.

3) *Decoding and Combination*: After obtaining the *a priori* LLRs  $\mathcal{L}_{dec}^{a,c}(c_{n,k}^{II})$  of the coded bits, which are the deinterleaved versions of  $\mathcal{L}_{dcp}^e(c_{n,k}^{II})$ , a typical soft decoder algorithm is employed in the DEC block of Fig 4 in order to generate the *extrinsic* LLRs  $\mathcal{L}_{dec}^{e,u}(b_{n,k}^{II})$  of the uncoded information bits by taking into account the *a priori* LLRs  $\mathcal{L}_{dec}^{a,u}(b_{n,k}^{II})$  of the uncoded information bits gleaned from the COM block of Fig 4. Then, the different versions of  $\mathcal{L}_{dec}^{e,u}(b_{n,k}^{II})$  received from the  $N$  relays are maximum ratio combined to yield an improved estimate of  $\mathcal{L}_{dec}^{a,u}(b_{n,k}^{II})$  by taking into account the soft LLRs obtained from the first transmission phase. In the feedback direction of Fig 4, the *a priori* LLRs  $\mathcal{L}_{dec}^{a,c}(c_{n,k}^{II})$  of the coded bits and the improved *a priori* LLRs  $\mathcal{L}_{dec}^{a,u}(b_{n,k}^{II})$  of the uncoded information bits gleaned from the output of the COM block of Fig 4 are used to yield the *extrinsic* LLRs  $\mathcal{L}_{dec}^{e,c}(c_{n,k}^{II})$  of the coded bits based on the corresponding soft decoding algorithm. After the last receiver iteration, the ultimate decision is made at the output of the COM block of Fig 4 by combining all the  $(N + 1)$  soft LLRs of the information bits.

#### IV. EXIT CHART ANALYSIS

##### A. Configurations and Assumptions

Let us now investigate the iterative decoding convergence behaviour of our receiver during the second phase in conjunction with different multiple source processing techniques with the aid of EXtrinsic Information Transfer (EXIT) charts [28], where we view the concatenation of the COM and DEC and the concatenation of the DCP and DET as our outer and inner code, as indicated by the dashed blocks of Fig 4. Before carrying out the EXIT chart analysis, we define the system parameters as follows:

- 1) We consider a  $K = N = 4$  MSC scenario, where all channels are AWGN channels. We assume that no decoding errors are imposed at the relay during the first phase source-to-relay transmissions, namely that we have perfect relaying. Furthermore, Remark 2 is obeyed. For the second transmission phase, an SNR per bit of  $\gamma_0^{II} = 6dB$  is assumed, while for the first phase source to destination transmission,  $\gamma_0^I = 0dB$  is assumed. For the iterative receiver at the destination, the first phase source-to-destination transmission contributes a fixed *a priori* information.

- 2) In the second phase, we maintain the same normalised throughput per relay node given by  $\eta = 1$  for all the three multiple source computation methods considered. Explicitly, for the CDM and CNC method having  $\eta_{cdm} = \eta_{cnc} = Kr$ , we let the channel code rate  $r = 1/K$ . For our VNC scheme, no channel codes are employed and all intermediate outputs of the VNC were enabled, namely we employed the  $r_1$ -VNC. Furthermore, in order to characterize the coding gain offered by the CNC and VNC schemes, we employ a repetition code as our channel coding scheme.

##### B. EXIT Curve

1) *Outer Code EXIT Curve*: Since the COM block may also be viewed as being equivalent to a repetition code of rate  $r = 1/N$ , when the CDM and CNC techniques are employed, the combined outer code is equivalent to a repetition code of rate  $r = 1/NK$ . When our VNC is considered, no DEC is employed, hence the combined outer code is equivalent to a repetition code of rate  $r = 1/N$ . Hence, the outer code may be interpreted as a variable node having  $(d_v + 1)$  edges, where  $d_v = 1/r$  and the additional edge is associated with the first phase direct source-to-destination transmission. As a result, the EXIT curve of the outer code may be formulated as [29]:

$$I_o^e(I_o^a, d_v, \gamma^I) = J \left( \sqrt{(d_v - 1)[J^{-1}(I_o^a)]^2 + \sigma_{ch}^2} \right), \quad (23)$$

where  $I_o^a$  and  $I_o^e$  denote the *a priori* and *extrinsic* mutual information of the outer code, respectively. Furthermore,  $\sigma_{ch} = 2/\sigma_D^I$  is the variance of the source-to-destination channel LLR values, where we have  $\sigma_D^I = \sqrt{1/2 \cdot 10^{\gamma_0^I/10}}$  for the uncoded first phase source-to-destination transmission [29]. Further elaborations on  $J(\cdot)$  may be found in the Appendix of [29].

2) *Inner Code EXIT Curve for the CNC and CDM Methods*: When CDM is considered, the EXIT curve of the composite inner code constituted by the CDM and DET blocks of Fig 4 may only be obtained by simulation, in order to determine the relationship of  $I_{cdm\&det}^e(I_{cdm\&det}^a, \gamma_0^{II})$ .

By contrast, the CNC method may be viewed as a  $d_c = K$ -degree check node having a total of  $(d_c + 1)$  edges, where the additional edge is connected to the DET block of Fig 4. The EXIT curve of a  $d_c$ -degree check node may be accurately (not exactly) approximated with the aid of the EXIT curve of the  $d_v = d_c$ -degree variable node in an AWGN scenario by exploiting their duality [29]. Hence, when considering the soft information passing from the CNC to the DET block, we have the EXIT curve relation [29] of:

$$I_{det}^a(I_{cnc}^a, d_c + 1) \approx 1 - J \left( \sqrt{d_c[J^{-1}(1 - I_{cnc}^a)]^2} \right), \quad (24)$$

where  $I_{det}^a$  and  $I_{cnc}^a$  denotes the *a priori* mutual information of DET and CNC. On the other hand, the EXIT curve relation for the soft information flow from the CNC to the outer code

is given by [29]:

$$I_{cnc}^e(I_{cnc}^a, I_{det}^e, d_c) \approx 1 - J \left( \sqrt{(d_c - 1)[J^{-1}(1 - I_{cnc}^a)]^2 + [J^{-1}(1 - I_{det}^e)]^2} \right), \quad (25)$$

where  $I_{det}^e$  and  $I_{cnc}^e$  denotes the *extrinsic* mutual information of DET and CNC. Furthermore, the EXIT curve of the DET block requires simulations in order to determine the relationship of  $I_{det}^e(I_{det}^a, \gamma_0^{II})$ . Hence the composite inner code EXIT curve of CNC is generated as:

$$I_{cnc\&det}^e(I_{cnc\&det}^a, \gamma_0^{II}, d_c) = I_{cnc}^e[I_{cnc\&det}^a, I_{det}^e(I_{det}^a, \gamma_0^{II}), d_c] \quad (26)$$

$$= I_{cnc}^e[I_{cnc\&det}^a, I_{det}^e(I_{det}^a(I_{cnc\&det}^a, d_c + 1), \gamma_0^{II}), d_c]. \quad (27)$$

3) *Inner Code EXIT Curve for the VNC Method:* The EXIT curve of VNC depends on the number of self-iterations employed, which affects the resultant combined EXIT curve of the VNC and DET blocks of Fig 4. Hence, we plot the EXIT curve of VNC for a sufficiently high number of self-iterations as the best-case benchmarker. The block of VNC seen in Fig 4 has two *a priori* inputs and two *extrinsic* outputs, hence conventional two-dimensional EXIT curves become incapable of describing the behaviour of the VNC. Therefore, we employ three-dimensional EXIT charts to visualise the iterative decoding convergence behaviour of our VNC.

We first draw the EXIT surface-I of the *extrinsic* output  $I_{vnc\&det}^e$  forwarded to the outer code as a function of two *a priori* inputs, namely of  $I_{vnc\&det}^a$  provided by the outer code and  $I_{det}^e$  provided by the DET block of Fig 4, as seen in Fig 6(a). We then draw the EXIT surface-II of the *extrinsic* output  $I_{det}^e$  provided for the DET block of Fig 4 as a function of two *a priori* inputs, namely of  $I_{vnc\&det}^a$  and  $I_{det}^e$  recorded from our simulations, as seen in Fig 6(b). We also draw the EXIT curve representing the *extrinsic* output  $I_{det}^e$  as a function of its *a priori* input  $I_{det}^a$  and then expand it into EXIT surface-III by incorporating another dimension, namely  $I_{vnc\&det}^a$ , which has no effect on the EXIT relationship between  $I_{det}^e$  and  $I_{det}^a$ , as demonstrated by the flat surface of Fig 6(c).

When having three EXIT surfaces, we first rotate EXIT surface-II by portraying  $I_{det}^e$  as a function of  $I_{vnc\&det}^a$  and  $I_{det}^a$ . The rotated EXIT surface-II is then plotted together with EXIT surface-III that has the same axes as seen in Fig 6(c). Given this arrangement, the curve of intersection between these two EXIT surfaces emerges. By recording the curve of intersection described by the three-triple  $\{I_{det}^a, I_{vnc\&det}^a, I_{det}^e\}$  and mapping them onto EXIT surface-I, we get  $I_{vnc\&det}^e$  with the two *a priori* inputs of  $I_{det}^e$  and  $I_{vnc\&det}^a$  provided by the curve of intersection. In this way, we obtain the relationship between  $I_{vnc\&det}^e$  and  $I_{vnc\&det}^a$  as the inner code's EXIT curve that subsumes the self iterations of our VNC and of the DET block.

### C. Convergence Analysis

Fig 6(d) and Fig 6(e) show the EXIT charts of the CDM technique and the CNC technique, respectively. Both schemes

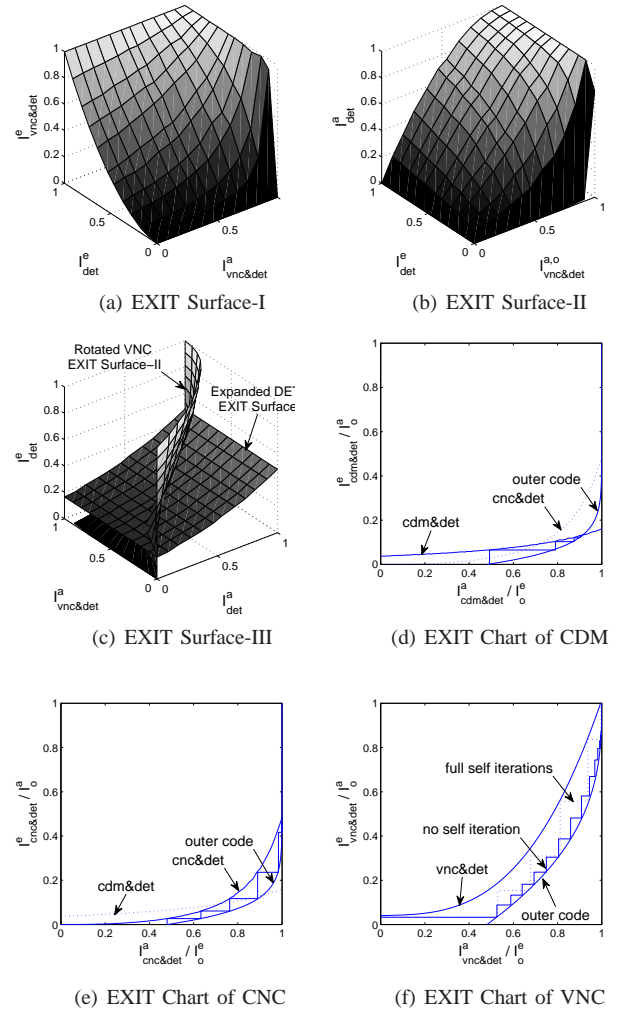


Fig. 6. The EXIT curves for various multiple source computation methods.

employ the same outer code, they hence have the same outer code EXIT curve. Observe in Fig 6(d) that the CDM method is unable to achieve iterative convergence, since we have an intersection between the inner code's and the outer code's EXIT curve. On the other hand, as seen in Fig 6(e), the CNC method is indeed capable of achieving decoding convergence. More explicitly, we can see that the EXIT curve of the CNC has a lower *extrinsic* mutual information in the low *a priori* mutual information region than that of the CDM, while it exhibits a significantly higher *extrinsic* mutual information in the high *a priori* mutual information region. This is the typical behaviour of check nodes, as explicitly described by the boxplus operation of Eq (14), which accumulates unreliable information, when only low *a priori* mutual information is available, while it provides a reliable output, when sufficiently reliable *a priori* mutual information is available. Note that the EXIT curve of the CNC method emerges from the origin, hence it fails to converge, if no first phase direct source-to-destination transmission is available. Hence, the information of the first phase may be viewed as the virtual *systematic* information part of CNC that assists the receiver in achieving convergence.

Fig 6(f) shows the EXIT curve of the  $r_1$ -VNC scheme em-

ploying a sufficiently high number of self-iterations, where the outer code's EXIT curve is obtained following the procedures introduced in Section IV-B.3. Under the assumptions made in Section IV-A, the VNC scheme is capable of achieving decoding convergence, since it reaches the EXIT chart's top right corner at the [1,1] point. Furthermore, we also recorded the Monte-Carlo simulation based decoder trajectories, when employing no self-iterations in VNC decoding and when employing a sufficiently high number of self-iterations during VNC decoding, which are represented by the stair-case-shaped solid trajectory and dotted trajectory, respectively. It can be seen in Fig 6(f) that both self-iteration configurations achieve convergence, where the arrangement using no self-iterations evolves the mutual information in its own way, embedded in the iteration loop constituted by the outer and inner code. Another important property is that the VNC EXIT curve is shifted upwards from the origin, implying the presence of useful non-zero *extrinsic* mutual information even when no *a priori* mutual information is available, hence the VNC method is capable of operating even without the first phase direct transmission.

## V. PERFORMANCE EVALUATION

### A. Configurations and Assumptions

Let us now present our simulation results for characterizing the various multiple source processing methods, where the following configurations and assumptions are made:

- 1) We consider a  $K = N = 4$  MSC scenario communicating over either AWGN channels or quasi-static flat Rayleigh fading channels. Remark 2 is obeyed and we assume  $E_b/N_0 = \gamma_0^I = \gamma_0^{II}$ .
- 2) During our simulations, the BLock Error Rate (BLER) versus  $E_b/N_0$  characteristics were recorded and each source had a packet length of  $N_b = 1024$ . For consistency, we employed the arrangement using no self-iterations for the decoding of VNC.
- 3) Apart from Fig 9, the second assumption stipulated in Section IV-A is also exploited.

1) *Effect of Iterations:* Fig 7 and Fig 8 show the beneficial effects of iterations at the destination receiver for various multiple source processing methods employed at the relays for both the AWGN channel and for a quasi-static Rayleigh fading channel, respectively. For the CDM and CNC methods, the attainable performance was recorded after  $\mathbb{I} = 15$  iterations, beyond which no further performance improvements may be achieved. The CDM method represented by the circle legends exhibits the worst performance, while the element-wise CNC technique characterized by the square legends is capable of attaining a significant coding gain of about 4dB for both the AWGN and for the quasi-static fading scenario at BLER of 0.001. When considering the proposed packet-wise VNC, we found that the performance of  $r_1$ -VNC relying on  $\mathbb{I} = 10$  iterations and denoted by the triangle legend is inferior to that of the CNC method. However, when  $\mathbb{I} = 15$  iterations are employed denoted by the rhombus legend, the VNC becomes superior in comparison to its CNC counterpart and a further performance gain of about 2dB is achieved for the AWGN

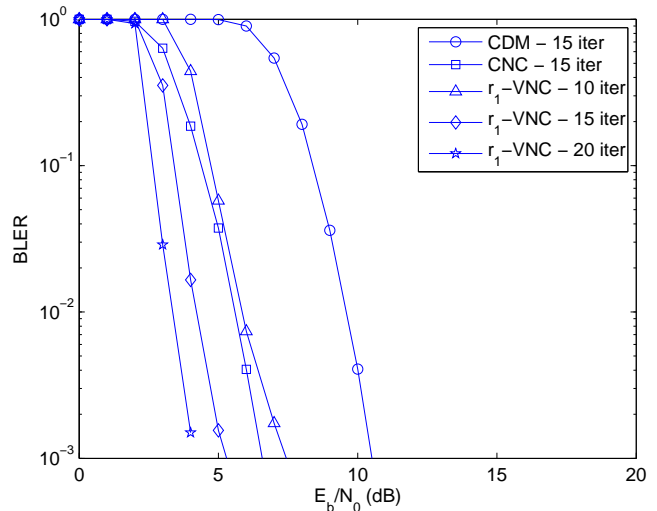


Fig. 7. The effect of iterations of the destination receiver for various multiple source computation methods employed at relay under AWGN channel conditions.

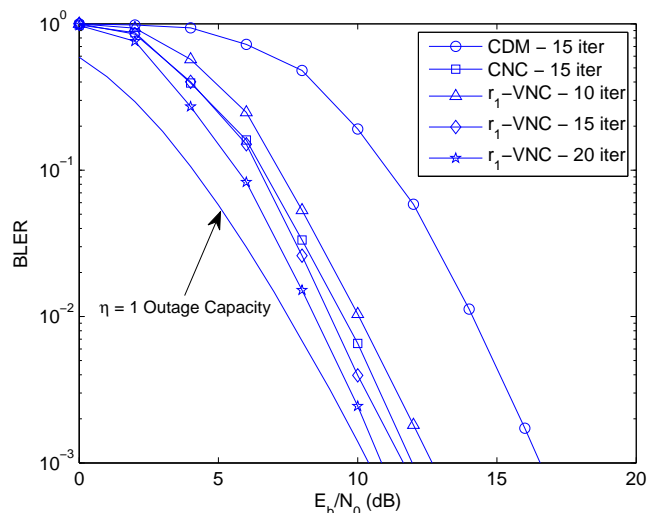


Fig. 8. The effect of iterations of the destination receiver for various multiple source computation methods employed at relay under quasi-static Rayleigh fading channel conditions.

case and 1dB for the quasi-static fading scenario, when using  $\mathbb{I} = 20$  iterations as indicated by the star legend in both figures at BLER of 0.001. Importantly, we also plot the outage capacity curve at a rate of  $\eta = 1$  for the quasi-static Rayleigh fading channel having a transmit diversity order of  $(N+1) = 5$  in Fig 8, where each of the  $N = 4$  diversity branches has a normalised power of  $P_n = 1/8$ , while the additional diversity branch has a normalised power of  $P^{II} = 1/2$ . It can be seen that the  $r_1$ -VNC using  $\mathbb{I} = 20$  iterations attains a BLER performance that is less than 1dB from the outage capacity without sophisticated joint channel and network coding.

2) *Effect of Variable Rate:* Fig 9 shows the BLER versus  $E_b/N_0$  performance of our VNC method for different number of intermediate outputs, namely for the  $r_1$ -VNC,  $r_2$ -VNC and  $r_4$ -VNC scenarios, when communicating over both AWGN

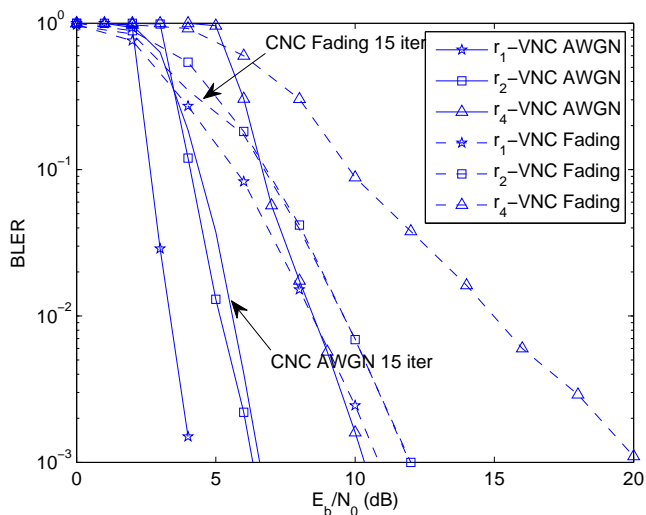


Fig. 9. Performance of  $r_1$ -VNC,  $r_2$ -VNC and  $r_4$ -VNC under both AWGN channel and quasi-static Rayleigh fading channel, where the destination receiver has 20 iterations.

and quasi-static Rayleigh fading channels, where the destination receiver uses  $\mathbb{I} = 20$  iterations. More explicitly, every second and every fourth intermediate outputs are enabled in the  $r_2$ -VNC and  $r_4$ -VNC schemes, respectively. Unsurprisingly, it can be seen in Fig 9 that increasing the normalised throughput per relay node by enabling less intermediate outputs leads to a BLER performance degradation for both channel conditions. Remarkably, the  $r_2$ -VNC method exhibits a similar BLER performance, when compared to the CNC method at a doubled normalised throughput per relay node under both AWGN and fading channel conditions.

3) *Effect of Relay Decoding Error:* Fig 10 shows the BLER versus  $E_b/N_0$  performance for our  $r_1$ -VNC method in the presence of first phase decoding errors during the source-to-relay transmissions, where the destination receiver uses  $\mathbb{I} = 20$  iterations. As discussed before, regardless of the specific first phase transceivers used, the source-to-relay transmissions result in potential decoding errors at the relay, which we characterize by assuming a Bit Error Probability (BEP) of  $P_e$ . It can be seen in Fig 10 that the ultimate BLER performance substantially degrades at  $P_e = 0.01$ , as denoted by the square legend. At  $P_e = 0.001$ , the BLER performance degrades only gently and it performs similarly to the CNC method. At  $P_e = 0.0001$ , only a marginal performance degradation is observed. These investigations suggest that if a powerful channel code is employed for the first phase transmission, the second phase transmissions may be safely activated. This is usually true for MSC, where the multiple sources are typically in each other's close proximity. On the other hand, when the instantaneous source-to-relay channel is severely faded, countermeasures for mitigating the effects of the relays' decoding errors have to be invoked [23].

## VI. CONCLUSION

In this paper, multiple source cooperation techniques were investigated, ranging from the classic CDM method to the

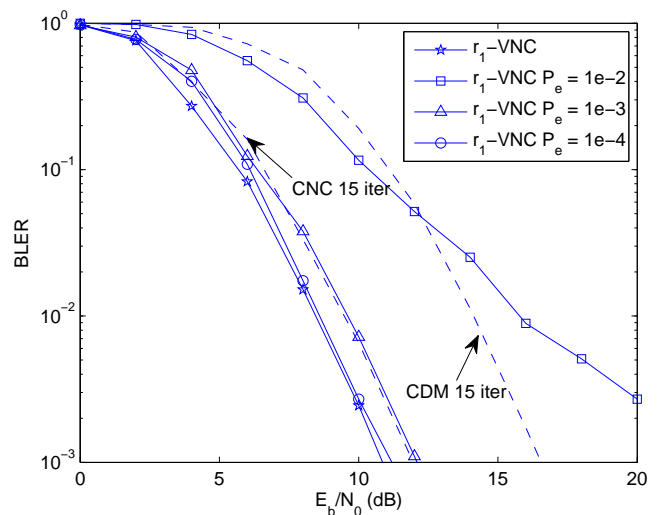


Fig. 10. The effect of decoding error of first phase source to relay transmission for  $r_1$ -VNC method, where the destination receiver has 20 iterations.

CNC method. We proposed a soft decoding method for CNC, which processes multiple information streams with the aid of factor graphs and the sum-product algorithm. A novel packet-wise VNC was also proposed, which is capable of operating at variable rates. Furthermore, the EXIT chart analysis of three different multiple source processing methods was carried out and their convergence behaviour was investigated. Our simulation results suggest that at the same normalised throughput per relay node, the CNC method using the sum-product algorithm is capable of providing a substantial coding gain over the CDM method. By contrast, the  $r_1$ -VNC technique is capable of further improving the BLER performance attained by CNC and approaches the outage capacity within 1dB. Hence, our proposed VNC provides a high flexibility and a near-optimal performance.

## REFERENCES

- [1] A. Sendonaris, E. Erkip, and B. Aazhang, "User cooperation diversity. Part I and II," *IEEE Transactions on Communications*, vol. 51, pp. 1927–1948, Nov. 2003.
- [2] J. N. Laneman and G. W. Wornell, "Distributed space-time coded protocols for exploiting cooperative diversity in wireless networks," *IEEE Transactions on Information Theory*, vol. 49, pp. 2415–2424, Oct. 2003.
- [3] M. Janani, A. Hedayat, T. E. Hunter, and A. Nosratinia, "Coded cooperation in wireless communications: space-time transmission and iterative decoding," *IEEE Transactions on Signal Processing*, vol. 52, pp. 362–371, Feb. 2004.
- [4] A. Nosratinia, T. E. Hunter, and A. Hedayat, "Cooperative communication in wireless networks," *IEEE Communications Magazine*, vol. 42, pp. 74–80, Oct. 2004.
- [5] T. Cover and J. Thomas, *Elements of Information Theory*. New York: Wiley, 2004.
- [6] A. K. Sadek, W. Su, and K. J. R. Liu, "Multinode cooperative communications in wireless networks," *IEEE Transactions on Signal Processing*, vol. 55, pp. 341–355, Jan. 2007.
- [7] B. Nazer and M. Gastpar, "Compute-and-forward: Harnessing interference through structured codes," *submitted to IEEE Transactions on Information Theory*. [Online]. Available: <http://arxiv.org/abs/0908.2119>
- [8] N. C. Tse and P. Viswanath, *Fundamentals of Wireless Communication*. Cambridge University Press, 2005.

TABLE I  
LIST OF IMPORTANT SYMBOLS.

General symbols	
$K, N$	number of sources and relays
$S_k, R_n, D$	source $k$ , relay $n$ and destination
$P, P_n$	total transmit power, transmit power of $R_n$
$P^I, P^{II}$	first and second phase transmit power
$N_b$	length of information bit vector
$N_c$	length of coded bit vector
$N_x$	length of transmit data vector
$r, b$	channel coding rate, bits per symbol
$W$	number of orthogonal channels
$\mathbb{I}, P_e, \Omega$	number of iterations, BEP and index set
$\eta_m$	normalised throughput for scheme 'm'
First phase operations of $S_k$	
$\mathbf{b}_k^I, \mathbf{x}_k^I$	information bit and transmit data vector
$\mathbf{y}_D^I, \mathbf{y}_n^I$	received signal vector at $D$ and $R_n$
$\mathbf{n}_{k,D}^I, \mathbf{n}_{k,n}^I$	noise vector at $D$ and $R_n$
$h_{k,D}^I, h_{k,n}^I$	channel between $S_k$ and $D$ , $S_k$ and $R_n$
Second phase operations of $R_n$	
$\mathbf{x}_{n,k}^{II}$	modulated data vector of $S_k$ for CDM
$\mathbf{c}_{n,k}^{II}$	coded bit vector of $S_k$ for CDM/CNC/VNC
$\mathbf{c}_{n,T}^{II}$	concatenated bit vector for VNC
$\mathbf{c}_n^{II}$	composite bit vector for CNC/VNC
$\mathbf{x}_n^{II}$	transmit data vector
$\mathbf{y}_D^{II}$	received signal vector at $D$
$\mathbf{n}_D^{II}$	noise vector at $D$
$h_{n,D}^{II}$	channel between $R_n$ and $D$
$f_{c,k}, f_m$	coding function and modulation function
Iterative processing for component 'm'	
$\mathcal{L}_m^e, \mathcal{L}_m^a$	<i>extrinsic</i> and <i>a priori</i> LLR
$I_m^e, I_m^a$	<i>extrinsic</i> and <i>a priori</i> mutual information
$d_v, d_c$	degree of variable nodes and check nodes

TABLE II  
LIST OF FREQUENTLY USED ABBREVIATIONS.

Frequently used abbreviations	
MSC	Multiple Source Cooperation
CDM	Code Division Multiplexing
CNC	Classic Network Coding
PNC	Physical-layer Network Coding
VNC	Variable-rate Network Coding
LLR	Logarithmic Likelihood Ratio
DET	DETECTION
DCP	DeComPosition
DEC	DECoder
COM	COMbiner
EXIT	EXtrinsic Information Transfer charts

[9] E. G. Larsson and B. R. Vojcic, "Cooperative transmit diversity based on superposition modulation," *IEEE Communications Letters*, vol. 9, pp. 778–780, Sept. 2005.

[10] R. Zhang and L. Hanzo, "Interleaved random space-time coding for multisource cooperations," *IEEE Transactions on Vehicular Technology*, vol. 58, pp. 2120–2125, May 2009.

[11] R. Ahlswede, N. Cai, S. Y. R. Li, and R. W. Yeung, "Network information flow," *IEEE Transactions on Information Theory*, vol. 4, pp. 1204–1216, Jul 2000.

[12] X. Bao and J. Li, "Matching code-on-graph with network-on-graph: Adaptive network coding for wireless relay networks," in *Proc. of Allerton Conf. on Commun., Control and Computing II*, Monticello, Ill, USA, Sept 2005, pp. 1568–1573.

[13] S. Zhang and S. C. Liew, "Applying physical-layer network coding in wireless networks," *EURASIP Journal on Wireless Communications and Networking*, vol. 2010, pp. 397–408, Feb 2010.

[14] T. Koike-Akino, P. Popovski, and V. Tarokh, "Optimized constellations for two-way wireless relaying with physical network coding," *IEEE Journal on Selected Areas in Communications*, vol. 27, pp. 773–787, June 2009.

[15] S. Zhang and S. C. Liew, "Channel coding and decoding in a relay system operated with physical-layer network coding," *IEEE Journal on Selected Areas in Communications*, vol. 27, pp. 788–796, June 2009.

[16] C. Hausl and J. Hagenauer, "Iterative network and channel decoding for the two-way relay channel," in *Proc. of IEEE International Conference on Communications*, Istanbul, Turkey, July 2006, pp. 1568–1573.

[17] L. Xiao, T. E. Fuja, J. Klierer, and D. J. Costello, "A network coding approach to cooperative diversity," *IEEE Transactions on Information Theory*, vol. 53, pp. 3714–3722, Oct 2007.

[18] G. Yue, X. Wang, Z. Yang, and A. Host-Madsen, "Coding schemes for user cooperation in low-power regimes," *IEEE Transactions on Signal Processing*, vol. 56, pp. 2035–2049, May 2008.

[19] O. Shalvi, "Multiple source cooperation diversity," *IEEE Communications Letters*, vol. 8, pp. 712–714, Dec. 2004.

[20] A. Ribeiro, R. Q. Wang, and G. B. Giannakis, "Multi-source cooperation with full-diversity spectral-efficiency and controllable-complexity," *IEEE Journal on Selected Areas in Communications*, vol. 25, pp. 415–425, Feb. 2007.

[21] R. Zhang and L. Hanzo, "Coding schemes for energy efficient multi-source cooperation aided uplink transmission," *IEEE Signal Processing Letters*, vol. 16, pp. 438–441, May 2009.

[22] S. Fong and R. Yeung, "Variable-rate linear network coding," *IEEE Transactions on Information Theory*, vol. 56, pp. 2618–2625, June 2010.

[23] K. C. Lee and L. Hanzo, "MIMO-assisted hard versus soft decoding-and-forwarding for network coding aided relaying systems," *IEEE Transactions on Wireless Communications*, vol. 8, pp. 376–385, Jan 2009.

[24] F. Kschischang, B. Frey, and H. Loeliger, "Factor graphs and the sum-product algorithm," *IEEE Transactions on Information Theory*, vol. 47, pp. 498–519, Feb. 2001.

[25] L. Hanzo, T. H. Liew, and B. L. Yeap, *Turbo Coding, Turbo Equalisation and Space-Time Coding for Transmission over Fading Channels*. Wiley-IEEE Press, 2002.

[26] M. C. Reed, C. B. Schlegel, P. D. Alexander, and J. A. Asenstorfer, "Iterative multiuser detection for CDMA with FEC: Near-single-user performance," *IEEE Transactions on Communications*, vol. 46, pp. 1693–1699, Dec. 1998.

[27] J. Hagenauer, E. Offer, and L. Papke, "Iterative decoding of binary block and convolutional codes," *IEEE Communications Magazine*, vol. 42, pp. 429–445, Mar. 1996.

[28] S. ten Brink, "Convergence behavior of iteratively decoded parallel concatenated codes," *IEEE Transactions on Communications*, vol. 49, pp. 1727–1737, Oct. 2001.

[29] S. ten Brink, G. Kramer, and A. Ashikhmin, "Design of low-density parity-check codes for modulation and detection," *IEEE Transactions on Communications*, vol. 52, pp. 670–678, Apr 2004.



**Rong Zhang** received his B.Eng. degree in communications engineering from Southeast University, Nanjing, China, in 2003 and his M.Sc. degree with distinction in radio frequency communications engineering and Ph.D. degree in wireless communications from the University of Southampton, United Kingdom, in 2005 and 2009, respectively. He was a system engineer with Mobile

Communications Division of China Telecom and is currently a research fellow with the Communications Research Group, School of Electronics and Computer Science, University of Southampton. He was awarded a joint EPSRC and Mobile VCE scholarship in 2006. His research interests include cellular networks optimization, multiuser communications, multi-antenna communications, and cooperative communications. He is a member of the IEEE and IET.



**Lajos Hanzo** FREng, FIEEE, FIET, DSc received his degree in electronics in 1976 and his doctorate in 1983. In 2009 he was awarded the honorary doctorate “Doctor Honoris Causa”. During his 35-year career in telecommunications he has held various research and academic posts in Hungary, Germany and the UK. Since 1986 he has been with the School of Elec-

tronics and Computer Science, University of Southampton, UK, where he holds the chair in telecommunications. He has co-authored 20 John Wiley - IEEE Press books on mobile radio communications totalling in excess of 10 000 pages, published about 970 research entries at IEEE Xplore, acted as TPC Chair of IEEE conferences, presented keynote lectures and been awarded a number of distinctions. Currently he is directing an academic research team, working on a range of research projects in the field of wireless multimedia communications sponsored by industry, the Engineering and Physical Sciences Research Council (EPSRC) UK, the European IST Programme and the Mobile Virtual Centre of Excellence (VCE), UK. He is an enthusiastic supporter of industrial and academic liaison and he offers a range of industrial courses. He is also a Governor of both the IEEE ComSoc and the VTS. He is the Editor-in-Chief of the IEEE Press and a Chaired Prof. also at Tsinghua University, Beijing. For further information on research in progress and associated publications please refer to <http://www-mobile.ecs.soton.ac.uk>